Influence of the Conditions in Pharmacophore Generation, Scoring, and 3D Database Search for Chemical Feature-Based Pharmacophore Models: One Application Study of ET_A- and ET_B-Selective Antagonists

Joan R. Cucarull-González,*,† Christian Laggner,‡ and Thierry Langer‡

Departament de Química, Universitat Autònoma de Barcelona, 08193 Bellaterra, Spain,
Department of Pharmaceutical Chemistry, Institute of Pharmacy, Center for Molecular Biosciences (CMBI),
University of Innsbruck, Innrain 52a, A-6020 Innsbruck, Austria

Received January 5, 2006

Using the commercial pharmacophore modeling suite Catalyst, we have studied the influence of the compare.scaledMultiBlobFeatureErrors .Catalyst parameter. The influence of this parameter has been studied in pharmacophore generation, hypothesis scoring, and database searching. This parameter, introduced in Catalyst 4.7, changed its default value in Catalyst 4.8, and it strongly influences the statistical quality of pharmacophore generation, scoring of the hypotheses, and database searching. Two different pharmacophore models have been constructed for the ET_A and ET_B receptor antagonists. Both models contain one positive ionizable, one negative ionizable, one hydrogen-bond acceptor, one hydrophobic aromatic, and one hydrophobic aliphatic feature. The models have been compared, and some differences in the position of the hydrogen-bond acceptor in the putative binding pocket have been highlighted.

INTRODUCTION

Following a recent study of our research group on the generation of chemical feature-based pharmacophore models for ligands of the angiotensin II receptor subtype 1 (AT_1),[1] we became interested in whether the presence of excluded volume spheres could improve the description of the pharmacophore model obtained previously. Therefore, we then studied the new HypoRefine algorithm implemented in version 4.9 of Catalyst, which is a widely used software package for automated pharmacophore model generation and virtual screening.[2] The Catalyst package version 4.9 includes three different methods of automatic generation of pharmacophore models: two quantitative modules (HypoGen and HypoRefine) and a third qualitative module (HipHop). This qualitative algorithm is useful when there is not enough affinity data for different compounds available, when all present similar affinities, or when they have a very close structural relationship.

METHODOLOGY

Because the original model had been generated with the HypoGen module of Catalyst 4.7, we repeated all the calculations using the 4.9 version of Catalyst. We built a new conformational model with the new program version, and then, using the same parameters as in the previous work, the automatic pharmacophore hypothesis generation was performed.

As a result, we obtained a pharmacophore that was different from the one of the original work. This new pharmacophore was, from a statistical point of view, less predictive than the previous one, as shown in Table 1. Although both pharmacophore models present the same features, the Δ cost is different, as is the relative arrangement of features in 3D space. The Δ cost is a measure of the statistical quality of the pharmacophore and is described extensively below. The two aligned pharmacophore models are depicted in Figure 1. According to this result, different Catalyst versions seem to lead to different pharmacophore models.

Table 1. Original AT_1 Receptor Pharmacophore Hypothesis (**I**) and Hypothesis Generated with the Default Settings of Catalyst 4.9 (**II**)

hypothesis	Δ cost	features[a]
I	63.426	1 HBA, 1 HyAl, 1 HyAr, 1 NegIo, 1 RA
II	59.400	1 HBA, 1 HyAl, 1 HyAr, 1 NegIo, 1 RA

[a] (HBA) hydrogen-bond acceptor, (HyAl) hydrophobic aliphatic, (HyAr) hydrophobic aromatic, (NegIo) negative ionizable, (RA) ring aromatic.

In light of these surprising results, we decided to look for the changes introduced in the software between the 4.7 and 4.9 versions that could affect the quality of the hypothesis. According to the official documentation,[3] the major changes that were introduced between versions 4.7 and 4.9 are as follows:

(i) The HypoRefine algorithm was added.

(ii) Improvement in the handling of excluded volume spheres was made.

(iii) The original iterative fitting algorithm was replaced with an analytical solution.

(iv) Improvements of the cis/trans amide bond proportion and the axial−equatorial distribution in 1,4-disubstituted piperidine rings during conformer generation were made.

* Corresponding author phone: +34 935814094; fax: +34 935811265; e-mail: joanramon.cucarull@uab.cat.
† Universitat Autònoma de Barcelona.
‡ University of Innsbruck.

10.1021/ci060006t CCC: $33.50
Published on Web 04/21/2006

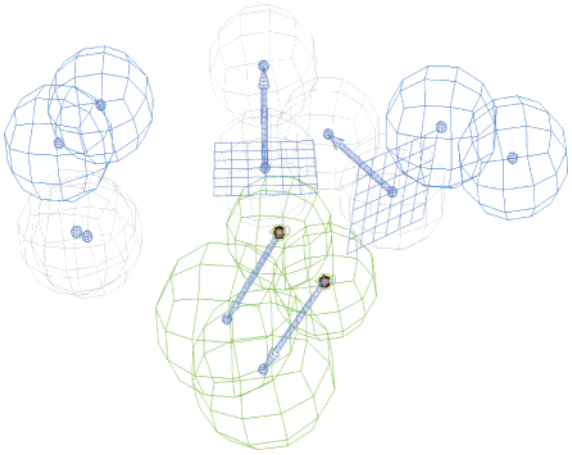

Figure 1. Comparison between the original pharmacophore model generated with Catalyst 4.7 (**I**) and the pharmacophore model generated with Catalyst 4.9 (**II**). Green spheres, HBA; blue, HyAl and HyAr; single gray sphere, NegIo; two gray spheres with plane and vector, RA. NegIo stands for negative ionizable.

Table 2. Original Pharmacophore Model (**I**) and Model Generated with the Default Configuration of Catalyst 4.9, Using the Conformational Model Previously Generated within Catalyst 4.7 (**III**)

hypothesis	Δ cost	features
I	63.426	1 HBA, 1 HyAl, 1 HyAr, 1 NegIo, 1 RA
III	59.951	1 HBA, 1 HyAl, 1 HyAr, 1 NegIo, 1 RA

(v) A change was made of the default value for the compare.scaledMultiBlobFeatureErrors parameter in the .Catalyst parameter file from FALSE in version 4.7 to TRUE in version 4.8 and later.

The addition of the HypoRefine algorithm had no effect on the final result because it was not used to generate this pharmacophore, as is the case with the improvement in the handling of excluded volume spheres.

The replacement of the fitting algorithm from an iterative to an analytical solution could influence the final result, but this influence should not be negative. Even more, these modifications cannot be undone by the setting of user-definable variables, so their influence cannot be studied.

We imagined that the other two modifications might influence the final result. To detect the influence of the modification of the conformational model, a hypothesis calculation was performed within Catalyst 4.9, using the original conformational model that had been generated with Catalyst 4.7.

When the original conformational model is used, the resulting hypothesis, presented in Table 2, is a little bit better than that generated using the conformational model generated with Catalyst 4.9, but its Δ cost value is still considerably lower than that of the original pharmacophore model.

The next step was to examine the influence of the value of the compare.scaledMultiBlobFeatureErrors parameter that can be set in the .Catalyst file, which resides in the user's home directory.

The compare.scaledMultiBlobFeatureErrors parameter was added in the Catalyst 4.7 release, and at that time, its default value was FALSE. In Catalyst 4.8, its default value was changed to TRUE. This parameter was introduced to avoid finding a negative fit value for a compound mapped to a hypothesis when multiblob features (i.e., features consisting of more than one sphere) are present in the hypothesis.

Table 3. Fit Value and Predicted Affinity Data for Compound **1** Mapped to Hypothesis **I**, with Different Settings for the compare.scaledMultiBlobFeatureErrors Parameter

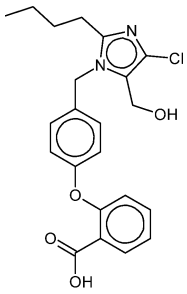

1

value	TRUE	FALSE
fit	10.72	6.03
affinity	0.0085	420

When a compound is mapped to a hypothesis, the quality of the mapping is expressed by the so-called fit value. This value is defined as the weight(f) × [1 − SSE(f)], where SSE(f) is the sum over location constraints c on f of $[(D(c)/T(c)]^2$, D is the displacement of the feature from the center of the location constraint, and T is the radius of the location constraint sphere for the feature (tolerance). Thus, the maximum fit value for a perfectly fitting compound is the sum over all the weight values for all features. The minimum value (no fit at all) should be 0, but because of the above formula, SSE(f) for a two-blob feature would be weight(f) × [1 − SSE(1) − SSE(2)], where SSE(x) is the error of the x blob, and because both SSE(1) and SSE(2) can take values from 0 to 1, the fit value can thus take negative values. To avoid this error, a new formula to estimate the fit for features consisting of two blobs (sum over all the mapped features f of weight(f) × {1 − 0.5[SSE(1) + SSE(2)]}) was introduced in Catalyst 4.7. However, with the compare.scaledMultiBlobFeatureErrors parameter set to FALSE, the default setting was to still use the old formula. Because the new formula (compare.scaledMultiBlobFeatureErrors value set to TRUE) considers only half of the sum of both errors, it can never give a negative fit value. It is worth mentioning that, with the new way of calculating the fit of the function in a feature, the fit value will always be equal to or higher than that with the old formula. Thus, this parameter strongly affects the fit value and the estimated activities of a compound, which are used during the pharmacophore model generation, affinity estimation, and database searching.

This effect can be seen by estimating the fit of the example compound **1**. The conformational model for this example was built with Catalyst 4.7 (compound number 12 in the original reference).[1] In both cases, this compound was mapped to pharmacophore model **I** with the compare/fit tool and with the settings "Best Fit", "Find Best Conformer", and "Maximum Omitted Features = 0".[4] Table 3 shows the different fit values of the compound mapped to the pharmacophore and the estimated affinity.

A pharmacophore model or hypothesis, as defined within the Catalyst package, is a collection of chemical features placed in 3D space that represent the most important

Table 4. Pharmacophore Models Generated with Different Conditions in Catalyst 4.9

	compare.scaledMultiBlobFeatureErrors	conformational model	configuration cost	Δ cost	features
I	FALSE[a]	Catalyst 4.7[a]	14.749	63.426	1 HBA, 1 HyAl, 1 HyAr, 1 NegIo, 1 RA
II	TRUE	Catalyst 4.9	14.979	59.400	1 HBA, 1 HyAl, 1 HyAr, 1 NegIo, 1 RA
III	TRUE	Catalyst 4.7	14.774	59.951	1 HBA, 1 HyAl, 1 HyAr, 1 NegIo, 1 RA
IV	FALSE	Catalyst 4.9	14.979	63.356	1 HBA, 1 HyAl, 1 HyAr, 1 NegIo, 1 RA
V	FALSE	Catalyst 4.7	14.774	60.635	1 HBA, 1 HyAl, 1 HyAr, 1 NegIo, 1 RA

[a] Original pharmacophore model generated with Catalyst 4.7.

characteristics of a drug to have a certain biological affinity. Catalyst uses chemical features that are not an atomistic description of the compound but a description of chemical properties.

In the quantitative algorithms (HypoGen and HypoRefine), the selection of a proper training set for the algorithm is a key point and will be described later on. In the Catalyst 4.8 release, the HypoGen algorithm has been extended to the HypoRefine algorithm. This HypoRefine algorithm allows Catalyst to automatically place excluded volume spheres—describing "forbidden zones" that the molecules must not fit—during the hypothesis generation.

The HypoGen run is divided into three phases. During the first one, known as the constructive phase, all the pharmacophore models which are common to the most active compounds are created. The second, called the subtractive phase, removes all the generated pharmacophore models in which the inactive compounds can fit. Finally, the third one, known as the optimization phase, makes some random modifications in the generated hypothesis—moving features, rotating vectors, or adding or removing features. Each modification is evaluated using the error cost value, and the best resulting hypotheses are reported.

These hypotheses are scored applying a so-called cost analysis. The total cost is calculated adding three partial cost values (error cost, weight cost and configuration cost). Catalyst also returns two important theoretical cost values, the null cost and the fixed cost. All of these cost values are represented in bits, and Catalyst analyzes the pharmacophore models using the Occam's razor principle; that is, among equivalent possibilities (hypotheses), the simplest (less bits cost) is the best. The fixed cost represents the simplest model that fits the data perfectly (perfect model), while the null cost represents a hypothesis with no features which estimates the affinity as the average affinity of all the compounds (no model at all). Because the null hypothesis is an "empty" hypothesis with no features, there is no contribution of the weight and configuration costs. The error cost is the most important part of the total cost and increases as the root-mean-square (RMS) difference between the estimated and the actual affinity for the training set increases. The RMS value is related to the quality of prediction of the hypothesis. The weight cost is a value that increases with the difference between the actual and ideal weights of the features. According to the documentation, the ideal value of the weight is 2 because higher weight values tend to force unrealistic conformations of the compounds to fit such features.

The configuration cost is a fixed cost that represents the complexity of the hypothesis space to be optimized. It describes the entropy of this space and is related to the number of hypotheses that have been created in the constructive phase and that survived the subtractive phase (s); thus, the configuration cost $= \log_2(s)$. This number should not be higher than 17, because Catalyst will otherwise truncate the hypothesis list, which leads to the problem that not all possible hypotheses are considered. Of course, the higher the configuration cost, the higher the number of hypotheses to be considered; thus, the computational time increases.

The cost of each hypothesis has a value between the fixed cost and the null cost. The higher the difference between the cost of the hypothesis and the null cost ($= \Delta$ cost), the higher the possibility that the hypothesis represents a true correlation. With a difference between the hypothesis cost and the null cost of 60 or more bits, there is an excellent possibility that the model represents a true correlation. With a difference of 40−60 bits, it is a chance of 75−90% that the hypothesis represents a good correlation. As the Δ cost value decreases, this possibility decreases too.

The error cost of a hypothesis depends on how good the correlation between the true affinity and the estimated affinity is. The estimated affinity is calculated using the fit value of the compound in each pharmacophore hypothesis. Thus, it is in the optimization phase where the compare.scaledMultiBlobFeatureErrors parameter influences the final results. HipHop does not have the optimization phase and is thus not affected by this parameter.

In this work, during the automatic hypothesis generation, both values of the compare.scaledMultiBlobFeatureErrors .Catalyst parameter—FALSE and TRUE—were studied in order to see their influence on the final pharmacophore model. The influence of the origin of the conformational models, generated with either Catalyst 4.7 or 4.9, was also studied.

As it can be seen in Table 4, the statistical significance of both hypotheses generated with the compare.scaledMultiBlobFeatureErrors parameter set to TRUE (default value in Catalyst 4.9; hypotheses **II** and **III**) is poorer than of those generated with the parameter set to FALSE (**IV**, **V**). Only the use of the FALSE value and the conformational model generated in Catalyst 4.9 lead to a pharmacophore model (**IV**) whose quality is similar to that of the one previously published. But if these two pharmacophore models (**I** and **IV**) are compared (Figure 2), it is clear that they are different because of their different spatial arrangements of features.

All the calculations performed using the same conformational model show the same configuration cost; that is, the configuration cost of the pharmacophore models generated with the conformational model obtained with Catalyst 4.7 is 14.774, and that of the conformational model generated with 4.9 is 14.979. Conformational models generated with Catalyst 4.9 lead to a configuration cost which is slightly higher, so more hypotheses are considered. The original

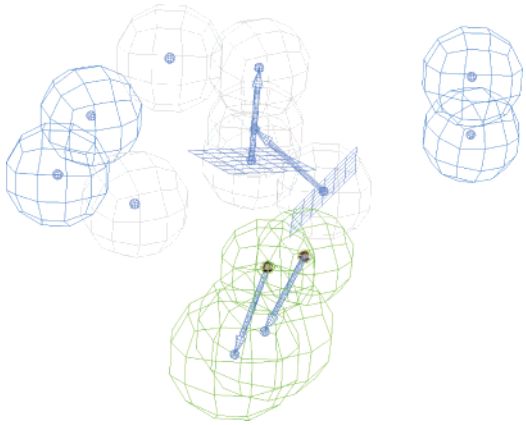

Figure 2. Comparison between the original pharmacophore (**I**) and the best one generated in Catalyst 4.9 (**IV**). Green spheres, HBA; blue, HyAr and HyAl; single gray sphere, NegIo; two spheres with plane and vector, RA.

Table 5. Scoring of the Training Set[a] for AT_1 Receptor Models

	compare.scaledMultiBlobFeatureErrors			
	FALSE		TRUE	
hypothesis	score	correlation	score	correlation
I	0.9223	0.9394	1.7859	0.9147
II	1.4222	0.9038	1.0345	0.9218
III	1.6437	0.8862	0.9854	0.9298
IV	0.8661	0.9515	1.7910	0.8832
V	0.9705	0.9318	1.5733	0.9278

[a] Conformational model for the training set built with Catalyst 4.7.

Table 6. Scoring of the Original Published Test Set[a] for AT_1 Receptor Models

	compare.scaledMultiBlobFeatureErrors			
	FALSE		TRUE	
hypothesis	score	correlation	score	correlation
I	1.4330	0.7786	2.2189	0.7809
II	1.6448	0.7025	1.4373	0.7427
III	2.3388	0.5537	2.1706	0.5839
IV	2.0674	0.5019	2.6099	0.5550
V	1.5353	0.7346	2.0167	0.7289

[a] Conformational model for the test set built with Catalyst 4.7.

configuration cost was 14.749, so in all the cases working with Catalyst 4.9, more hypotheses are considered. The compare.scaledMultiBlobFeatureErrors parameter does not affect the configuration cost because, as previously mentioned, the configuration cost is calculated during the subtractive phase and the parameter is applied during the later optimization phase.

The quality of the hypotheses depends on the fit of the compounds that are included in the training set, which is calculated during the hypothesis generation. Thus, the value of the compare.scaledMultiBlobFeatureErrors parameter should affect the hypothesis' real cost and correlation. We also studied the ability of these different pharmacophore models to predict the affinities for a test set. The data of scoring the hypotheses against the training set with different values for the compare.scaledMultiBlobFeatureErrors parameter is presented in Table 5. In Table 6, the hypotheses are scored against the test set also considering both values of the parameter. In both series, the compare.maxOmittedFeaturesFast parameter was set to 2. The score is a measure of how precisely the estimated activities fit the true ones: the lower the score, the better the activity estimation.

Table 7. Number of Hits for Database Searches with Different Values for the compare.scaledMultiBlobFeatureErrors Parameter

	compare.scaledMultiBlobFeatureErrors	
hypothesis	TRUE	FALSE
I	26	23
II	24	20
III	28	27
IV	17	13
V	24	22

From Table 5, we can see that the best results obtained in the score hypothesis against the training set, related to score and correlation, are obtained using the same value in the Catalyst compare.scaledMultiBlobFeatureErrors parameter that was used during the automatic hypothesis generation. This is not surprising, considering the fact that the hypotheses that were returned by the automatic hypothesis generation process are those that showed the best correlation under the given settings—thus, one would expect that the hypotheses are somewhat optimized toward these settings. The origin of the conformational models seems to have no clear influence on the final results. The overall best hypothesis regarding the "score hypothesis" results is hypothesis **IV**, which also has the best value for cost among the new models.

Table 6 shows that, most of the time, the best results for scoring the hypothesis against the test set are obtained using the TRUE value for the compare.scaledMultiBlobFeatureErrors parameter. These results do not parallel the results obtained while scoring against the training set. Again, scoring against the test set seems to imply that the origin of the conformational model is not important.

The overall best hypothesis regarding the score hypothesis results against the test set is the original hypothesis **I**, the best in pharmacophore generation, while **IV** performs the worst for both values.

The other process that is affected by the value of the compare.scaledMultiBlobFeatureErrors parameter is the virtual screening of 3D databases. During database searching, all the compounds are mapped into the hypothesis, and the fit value of the mapping will depend on the value of this parameter. That means that different numbers of hits can be retrieved with different values for this parameter. To check this point, we used a subset of the Derwent World Drug Index (WDI), restricted to 66 compounds used in the original work where only 25 compounds were found to map the original hypothesis (Table 7).

It can be clearly seen that the number of hits is always higher when the parameter is set to TRUE than it is when it is set to FALSE. This effect can be explained by the fact that, when the TRUE value is used, the error of mapping a function to a feature is lower; thus, the fit is higher. This effect is observed in all of the cases regardless of the origin of the pharmacophore model.

To state that the dependence on this value was the general tendency rather than an exception, we did the same studies in other cases, namely, pharmacophore models for inhibitors of dihydrofolate reductase (DHFR) from *Mycobacterium avium* and its human analogue[5] as well as models for the endothelin receptors.[6] Finally, to state the utility of this parameter in a new work, ET_A- and ET_B-selective endothelin

Table 8. Statistical Data of Pharmacophore Models for MAC DHFR Generated under Different Conditions

compare.scaledMultiBlobFeatureErrors	Δ cost	features[a]
original (**VI**)	51.820	HBA, HBA, Hy, RA
FALSE (**VII**)	53.365	HBD, HBD, Hy, RA
TRUE (**VIII**)	52.369	HBD, HBD, Hy, RA

[a] Hy, hydrophobic feature.

Table 9. Statistical Data for Pharmacophore Models of hDHFR Generated under Different Conditions

compare.scaledMultiBlobFeatureErrors	Δ cost	features
original (**IX**)	51.931	HBD, HBD, HBD, Hy
FALSE (**X**)	52.534	HBD, HBD, HBD, Hy
TRUE (**XI**)	50.950	HBD, HBD, HBD, Hy

receptor antagonist pharmacophore models were created observing the effect of the values for this parameter.

PHARMACOPHORE MODELS FOR DIHYDROFOLATE REDUCTASE

The original work about inhibitors of the dihydrofolate reductase complex from *M. avium* (MAC DHFR) and its human analogue (hDHFR) includes two training sets, one for MAC DHFR and another one for hDHFR. Because the original conformational model built with Catalyst version 4.6 was not available, a new conformational model was generated on the basis of the structures presented in the publication, and the calculations done to generate the hypothesis were performed using both values for the compare.scaledMultiBlobFeatureErrors parameter.

In the case of MAC DHFR, Catalyst was allowed to find a minimum number of 0 and a maximum number of 2 features of each of the following features: hydrogen-bond donor (HBD), hydrogen-bond acceptor (HBA), hydrophobic (Hy), and ring aromatic (RA). In the case of hDHFR, a minimum number of 0 and a maximum number of 3 was allowed for the same features.

Regarding the results for MAC DHFR displayed in Table 8, the most outstanding point that arises is that the pharmacophore models are composed of different features. The two best hypotheses, which are the ones newly generated in this work, present two hydrogen-bond donor features, one hydrophobic feature, and one ring aromatic feature. The original best pharmacophore consists of two hydrogen-bond acceptor features instead of two hydrogen-bond donors, one hydrophobic feature, and one ring aromatic feature.

If the 10 best original hypotheses reported are checked for all three cases, we can see that some contain two hydrogen-bond donor features, others contain one hydrogen-bond donor and one acceptor, and others contain two hydrogen-bond acceptors. It seems that different versions of the program may reorder the quality of the hypotheses.

The next point is that both pharmacophore models generated with the new Catalyst version are better—regarding the statistical significance—than the original one, the best having compare.scaledMultiBlobFeatureErrors set to FALSE.

Both hDHFR hypotheses—presented in Table 9—comprise the same features as those in the original work. However, in this case, the new pharmacophore model generated with compare.scaledMultiBlobFeatureErrors set to TRUE (**XI**) has the lowest cost value. As in the previous case, the one generated with Catalyst 4.9 using the FALSE (**X**) value shows the most favorable Δ cost value. Thus, this example confirms the results obtained for MAC DHFR.

Table 10. Results of Scoring the Hypotheses for MAC DHFR against the Training Set Taken from Table 1 in the Original Work

	compare.scaledMultiBlobFeatureErrors			
	FALSE		TRUE	
hypothesis	score	correlation	score	correlation
VII	0.7540	0.9628	1.5676	0.9406
VIII	1.5369	0.9435	0.9504	0.9393

Table 11. Results of Scoring the Hypotheses for hDHFR against the Training Set Taken from Table 3 in the Original Work

	compare.scaledMultiBlobFeatureErrors			
	FALSE		TRUE	
hypothesis	score	correlation	score	correlation
X	0.5769	0.9781	1.2237	0.9548
XI	1.3882	0.9738	0.7007	0.9669

Table 12. Results of Scoring the Hypothesis of MAC DHFR against the Test Set Taken from Table 5 in the Original Work

	compare.scaledMultiBlobFeatureErrors			
	FALSE		TRUE	
hypothesis	score	correlation	score	correlation
VII	2.3876	0.6385	1.3238	0.6000
VIII	3.0092	0.6672	1.4716	0.6300

Table 13. Results of Scoring the Hypothesis of hDHFR against the Test Set Taken from Table 5 in the Original Work

	compare.scaledMultiBlobFeatureErrors			
	FALSE		TRUE	
hypothesis	score	correlation	score	correlation
X	6.1392	0.4517	6.2064	0.4400
XI	6.2601	0.4492	6.1700	0.4354

The next step was to check the differences at scoring the newly generated hypotheses against their training sets with different settings of the compare.scaledMultiBlobFeatureErrors parameter. These results are presented in Table 10 for MAC DHFR and in Table 11 for hDHFR. In both cases, the parameter compare.maxOmittedFeaturesFast was set to 2.

Not following the same tendencies observed for the AT_1 models, the best scoring results are not obtained when working under the same conditions as those under which the hypotheses were created. However, in both DHFR cases, the correlation is always better using the FALSE value in the compare.scaledMultiBlobFeatureErrors parameter, although with only small differences.

The next step was to score both pharmacophore models against their test sets published in the original work. The results for both cases are depicted in Tables 12 and 13.

Following the tendencies observed during scoring against the training set, in both pharmacophore models, the best results are obtained with the FALSE value in the compare.scaledMultiBlobFeatureErrors parameter, in contrast to the case of AT_1 where the best correlation was found using the same value as that in pharmacophore model generation.

Recently, a homology modeling study between the known *Mycobaterium tuberculosis* DHFR crystal structure (PDB

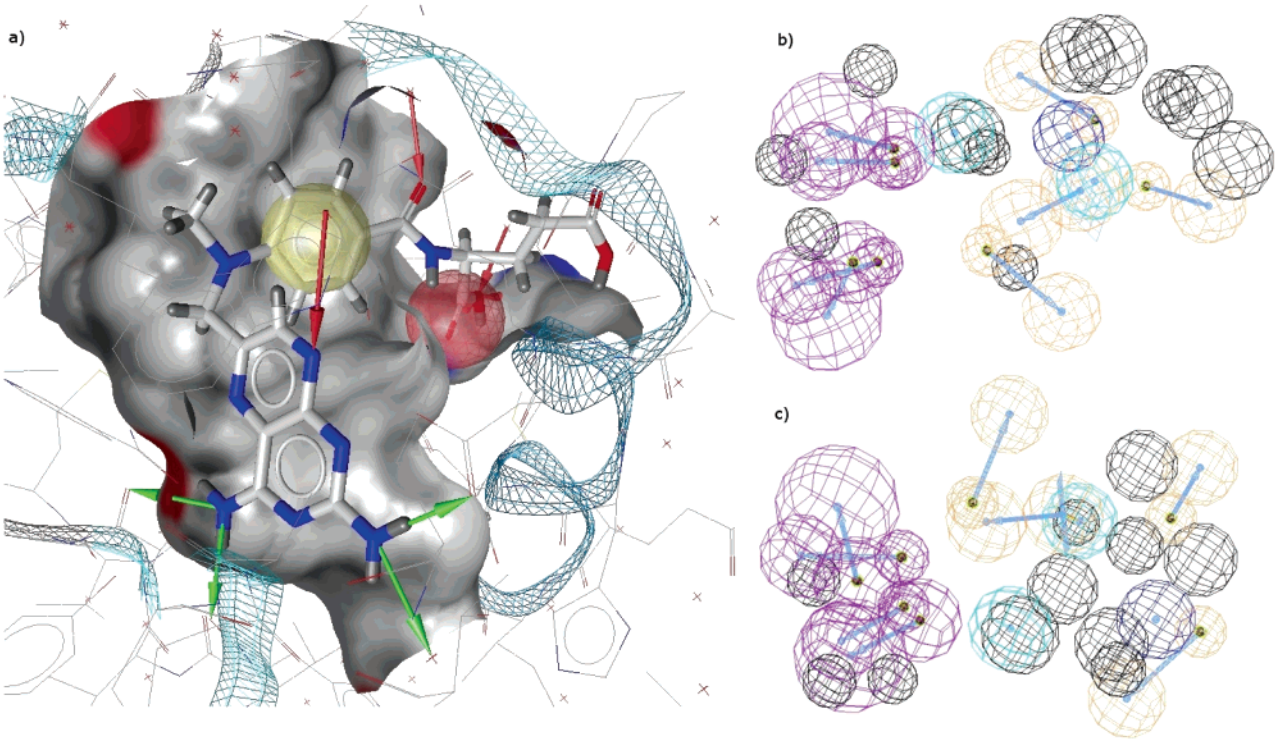

Figure 3. (a) Methotrexate interaction with the host extracted with LigandScout. Red arrows, HBA-F; green arrows, HBD; yellow sphere, Ar; red sphere, NegIo. (b) Hypothesis **VIII** mapped with the model from 1DF7. (c) Hypothesis **VII** mapped with the model from 1DF7. In b and c, the HBD (magenta) maps similarly but with different directions and the RA (brown) and Ar (blue) also map quite good. In both cases, the Hy feature overlaps with an Xvol. The rest of the brown multiblob features are HBA-F.

1DF7)[7] and the known sequence of the MAC DHFR has been published.[8] This work showed that both binding sites were similar.

To estimate the quality of the pharmacophores generated in this work, it is possible to compare these pharmacophore models and the one obtained directly from the crystal. To extract the model from the crystal, the LigandScout[9] software was used. This software extracts the information from the interaction of the ligand bound in the receptor and the surrounding amino acids. The extracted model consists of 1 Hy, 1 NegIo, 2 HBD, 3 HBA-F, and 11 excluded volumes (Xvol). An image of the interaction between the ligand and the host is shown in Figure 3a.

When this pharmacophore model is compared to the MAC DHFR models obtained in this work, the first main difference is the number of features that the models have. Catalyst can only add up to five features to a hypothesis when working with HypoGen. The models obtained in this work have four features, and the model from the crystal structure has seven features.

The mapping between pharmacophore model **VIII** and the model from 1DF7 is shown in Figure 3b. Figure 3c shows the mapping between hypothesis **VII** and 1DF7. When the models are compared, the common features map well, except 1 Hy, which maps an excluded volume, and both models describe well the twist between the aromatic moieties.

PHARMACOPHORE MODELS FOR ET_A AND ET_B RECEPTOR ANTAGONISTS

Endothelins (ET-1, ET-2, and ET-3), discovered in 1988,[10] are 21-residue amino acid bicyclic peptides. These peptides are the most potent vasoconstrictors known today (ET-1 is 10-fold stronger than angiotensin) and are also potent mitogens. Soon after their discovery, two receptors subtypes were found, termed ET_A and ET_B.

Endothelins act by binding to a family of membrane-associated G-protein-coupled receptors. When ET-1 binds to ET_A, it starts a cascade leading to vasoconstriction. When it binds to ET_B, the effects are not totally clear yet, but they seem to be related to the vasodilatory response to endothelins via the release of nitric oxide. The ET_A receptor is present in the vascular smooth muscle, lung, aorta, and heart, while the ET_B receptor is present in the endothelium, cerebral cortex, cerebellum, liver, kidney, lung, and placenta.

Endothelins are involved in some vascular diseases such as hypertension, congestive heart failure, vasospasm, restenosis following angioplasty, subarachnoid hemorrahage, iscemia, pulmonary hypertension, and renal failure.

EARLIER APPROACHES

Since the discovery of endothelins, several 3D-QSAR studies have been published about endothelin antagonists.[11] Although these studies were done with several structural families—different from the one we are working with here—all of them present a pharmacophore model that includes one negative and one positive ionizable or charged feature. Apart from that, the pharmacophore models also contain some hydrophobic areas, and some contain excluded volume spheres or areas that need a bulky group. The group that has published the compounds that we have used for our own studies has presented some SAR analysis[12] to discriminate between the ET_A and ET_B receptor, and according to this, it seems that the presence of a hydrogen-bond acceptor in the side chain plays an important role in discriminating between ET_A and ET_B receptors.

Table 14. Statistical Data for Endothelin-A Antagonist Pharmacophore Models Generated under Different Conditions

hypothesis	conformational model	compare.scaledMultiBlobFeatureErrors	Δ cost	features
XII	original, 4.7	original, FALSE	49.440	HBA HY HY NegIo RA
XIII	4.7	FALSE	49.650	HBA HY HY NegIo RA
XIV	4.9	FALSE	49.714	HBA HY HY NegIo RA
XV	4.7	TRUE	45.960	HBA HY HY NegIo RA
XVI	4.9	TRUE	50.018	HBA HY HY NegIo RA

In a recent work[6] of our research group dealing with endothelin-A-selective receptor antagonists, a chemical-function-based pharmacophore was generated including two hydrophobic, one hydrogen-bond acceptor, and one negative ionizable feature. This work is used here only to test against the effect of the value of the compare.scaledMultiBlobFeatureErrors parameter. Because it is important to discriminate between both receptors, the aim of the second example concerning endothelin antagonists is to generate two different pharmacophore models for the endothelin receptor antagonists, one for the ET_A receptor and a second one for the ET_B receptor, based on common features of compounds that present a wide range of affinity against these receptors. Once these two pharmacophore models are obtained, we can compare both and try to see the differences in the location of critical interaction sites.

PHARMACOPHORE MODELS FOR ENDOTHELIN-A ANTAGONISTS

In the original work,[6] two HypoGen runs were performed because the configuration cost of the first calculated hypothesis exceeded 17 bits, so Catalyst truncated the list of available hypotheses, and not all of the possible hypotheses were considered. Because this elimination of hypotheses can distort the results we are studying, only the second run of the original work is considered.

A new conformational model and hypothesis were generated using the same conditions described in the published work, allowing Catalyst to find exactly two hydrophobic features and one of each of the following: hydrogen-bond acceptor, ring aromatic, and negative ionizable.

In this case, the different conditions are listed in Table 14, and the best result is the one using the conformational model generated with Catalyst 4.9 and compare.scaledMultiBlobFeatureErrors set to TRUE (**XVI**). There is a small difference (about 0.3 bits) between the best and the second best hypothesis, which uses the FALSE value and the conformational model generated with Catalyst 4.9 (**XIV**). The worst results are always those using the conformational model generated with Catalyst 4.7.

After that, these four hypotheses were scored against their training set. The results obtained regarding the different values for the compare.scaledMultiBlobFeatureErrors parameter are presented in Table 15.

Again, it can be observed that the best correlation and score are obtained when the "score hypothesis" operation is performed with the same compare.scaledMultiBlobFeatureErrors value used during pharmacophore generation.

Then, the hypotheses were scored against the original test set[6] generated with Catalyst 4.7. The scoring was performed considering both values in the compare.scaledMultiBlobFeatureErrors parameter (Table 16).

Although all of the correlation values are rather low, the best result is obtained using the conformational model generated with Catalyst 4.7 and the TRUE value in the compare.scaledMultiBlobFeatureErrors parameter (**XV**), which is the worst model regarding the pharmacophore generation output data. In three out of four times, the best results are obtained using the FALSE value during hypothesis scoring.

Table 15. Results of Scoring Different Endothelin-A Antagonist Hypotheses against Each Training Set

	compare.scaledMultiBlobFeatureErrors			
	FALSE		TRUE	
hypothesis	score	correlation	score	correlation
XII	0.5806	0.9880	2.1606	0.9616
XIII	1.5417	0.9115	1.7522	0.8951
XIV	1.0072	0.9388	1.3218	0.9136
XV	1.5694	0.8892	1.1189	0.9171
XVI	1.5075	0.9174	0.9175	0.9453

Table 16. Results of Scoring Different Endothelin-A Antagonist Hypotheses against the Test Set Built with Catalyst 4.7

	compare.scaledMultiBlobFeatureErrors			
	FALSE		TRUE	
hypothesis	score	correlation	score	correlation
XII	2.3717	0.6075	2.2281	0.5794
XIII	2.9030	0.2064	2.8356	0.2146
XIV	2.8160	0.4312	2.5156	0.3925
XV	5.2505	0.6734	4.7562	0.6437
XVI	3.4344	0.4536	2.7932	0.4151

Finally, to demonstrate the utility of this parameter, a study of endothelin A and B antagonists is performed considering both values of the compare.scaledMultiBlobFeatureErrors parameter.

GENERAL METHODOLOGY

The selection of the training set is a key step in automatic pharmacophore generation. Because the generated pharmacophore can only be as good as the input data set used to perform the calculation, it is important to follow some guidelines to achieve a statistically sound and predictive model.

According to the developer,[13] for a quantitative approach with HypoGen, the minimum number of compounds to be introduced as a training set should be 16. These compounds should span an affinity range of 4−5 orders of magnitude. The most active compound known must always be included in the training set. Each order of magnitude needs to be represented by at least three compounds. Each compound presented in the training set should give some important information about the type, number, and spatial arrangement of the interaction sites. This information should not be repeated in order to avoid redundancy. If two compounds are structurally similar and have similar affinities, only the most active should be included.[14] If they present different affinities, both can be chosen.

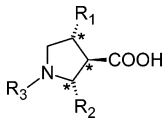

Figure 4. Pyrrolidine core.

It is also necessary that all of the compounds bind at the same binding site and that the affinity data is obtained in a comparable way. In the present study, all the data were obtained from MMQ cells (known to contain ET_A receptors) and porcine cerebellar tissues (known to contain ET_B receptors) as reported elsewhere.[12,18] The uncertainty value associated with these data was set to the default value 3, which is appropriate for most assays. This value represents the ratio between the reported value and the minimum and maximum values for the true affinity. The uncertainty is used to determinate which compounds are used as the most active in the constructive phase to generate the first set of hypotheses.

Catalyst uses a modified version of the CHARMM force field together with the Poling[15] algorithm for generating the conformational model. This algorithm ensures good coverage and little redundancy of the conformational space by forcing similar conformers away from each other and has been shown to yield conformational models containing the biologically active conformation if the energy threshold is set to 20 kcal/mol above the calculated global minimum energy.[16]

To create a conformational model in the Catalyst package that can be used as a template for automatic pharmacophore generation, we used the BEST method and up to 255 conformers. All the other parameters were kept at their default values. In our case, all compounds contain three stereocenters in the pyrrolidine ring, as shown in Figure 4. According to the explained synthetic route in the original works, these stereocenters always show a trans−trans relative stereochemistry as depicted in Figure 3. Most of those compounds are not enantiomerically pure but are racemic mixtures.

Therefore, we were interested in generating a conformational model which describes both kinds of compounds (racemic and enantiopure). While drawing structures in Catalyst, relative stereochemistry can be set, which means that Catalyst generates a conformational model with only this relative stereochemistry, but with all possibilities regarding absolute stereochemistry.

When we attempted to do so under standard conditions, Catalyst generated conformers of both possible isomers, but not half of the conformers from one isomer and half from the other. For us, this was not a good description of the conformational model.

There is one .Catalyst parameter which avoids erasing similar conformers called confAnalysis.skipStereoIsomerMirrorImages. In its default value, TRUE, if there are two conformers that are mirror images, Catalyst erases one of them. If it is set to FALSE, Catalyst keeps both conformers.

When this parameter was set to FALSE, the results were not better, as shown in Table 17, because only 2 out of 19 compounds presented a difference of occurrence (enrichment) between both enantiomers lower than 10%. Table 17 shows a collection of compounds with the difference in the occurrence of each enantiomer.

Table 17. Ratio between Conformers that Show the Same or Mirror Stereochemistry of the Initially Entered Structure[a]

compound	drawn	mirror	enrichment
9	62	17	72.6
12	37	72	−94.6
14	61	66	−8.2
15	66	41	37.9
19	55	35	36.4
20	33	80	−142.4
21	93	34	63.4
27	78	32	59.0
29	94	32	66.0
30	51	51	0.0
34	46	56	−21.7
37	49	78	−59.2
39	63	19	69.8
43	53	64	−20.8
48	82	45	45.1
52	34	89	−161.8
55	64	3	95.3
58	38	89	−134.2
97	31	40	−29.0

[a] Enrichment is calculated as $100(D - M)/D$ and should ideally be 0.

Another solution to properly describe these mirror images seemed to be the use of the catHypo.forceAbsoluteStereochemistry parameter. When it is set to 0 (default value), Catalyst considers the conformers generated and their mirror images during automated pharmacophore generation. When it is set to 1, only the drawn stereochemistry is considered. Unfortunately, using the 0 value, we were losing information from those compounds in the training set that were enantiopure, which was not acceptable for us.

Because these options were not satisfactory, we decided to leave all .Catalyst parameters at their default values, except catHypo.forceAbsoluteStereochemistry, which was set to 1, and built the conformational models for the enantiopure compounds with up to 255 conformers. For the racemic compounds, however, we built a 127-conformer model, setting relative stereochemistry, and then created its mirror images (by changing the sign of the coordinates) with a program written in Java. To generate the 127 conformations, we first built a model of up to 255 conformers with the BEST method. After that, a second conformational model calculation was run allowing up to 127 maximum conformers. This way, we ensured that we would always get the maximum 127 conformers. If the software was allowed to generate up to 127 conformers right from the beginning, we observed that, many times, this number of conformers was not achieved.

GENERATION OF PHARMACOPHORE HYPOTHESES

The next important step in automated hypothesis generation is the selection of possible features and the number of occurrences allowed for each of them. As described above, previous works show that the pharmacophore model must contain hydrophobic areas (in the present work, separated into aromatic and aliphatic hydrophobic features), some charged areas, and hydrogen-bond acceptors.

Because we were interested in comparing the two obtained pharmacophore models, both pharmacophore generation processes were performed under the same conditions (i.e., allowing the same kind and number of features).

Table 18. ET_A Training Set[a]

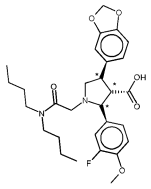

(±)-**2**

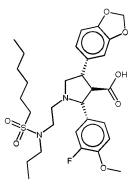

3

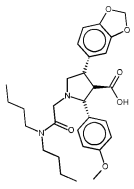

4

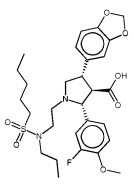

5

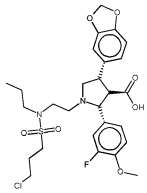

6

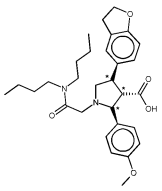

(±)-**7**

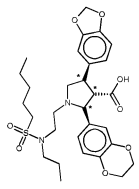

(±)-**8**

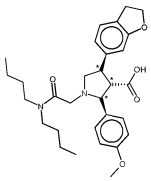

(±)-**9**

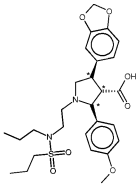

(±)-**10**

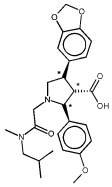

(±)-**11**

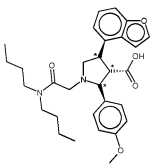

(±)-**12**

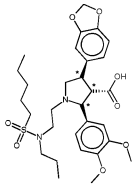

(±)-**13**

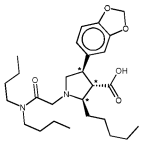

(±)-**14**

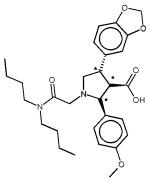

(±)-**15**

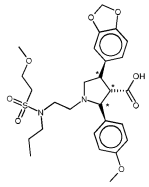

(±)-**16**

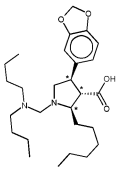

(±)-**17**

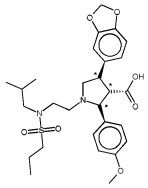

(±)-**18**

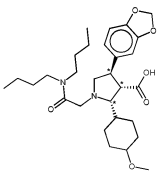

(±)-**19**

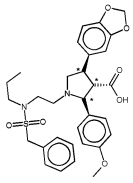

(±)-**20**

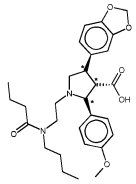

(±)-**21**

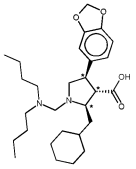

(±)-**22**

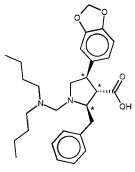

(±)-**23**

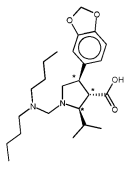

(±)-**24**

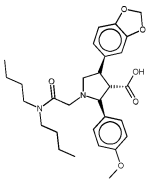

25

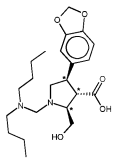

(±)-**26**

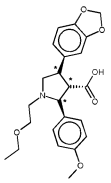

(±)-**27**

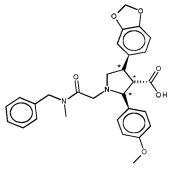

(±)-**28**

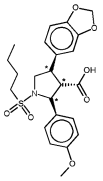

(±)-**29**

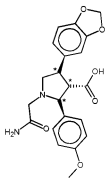

(±)-**30**

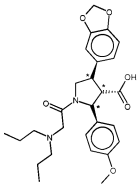

(±)-**31**

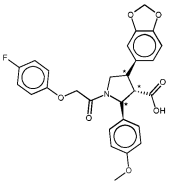

(±)-**32**

[a] The * means that the stereocenters keep the relative stereochemistry and they are racemic mixtures as indicated by (±). The unmarked compounds are enantiopure and possess the drawn stereochemistry.

We allowed Catalyst to find between one and two of each of the following features: hydrogen-bond acceptors, hydrophobic aromatic, and hydrophobic aliphatic. And we allowed Catalyst to find only one negative ionizable and one positive ionizable feature.

To achieve more accurate results while performing the automatic hypothesis generation, some .Catalyst parameters were modified. These modified parameters are catHypo.forceAbsoluteStereochemistry = 1 and compare.considerMirror = 0.[17] Furthermore, the effect of the two possible settings for the compare.scaledMultiBlobFeatureErrors parameter was studied.

MODELS FOR THE ET_A RECEPTOR

A 31-compound training set was carefully selected from the literature[12,18] to cover a wide space of diversity within this structural class according to the guidelines stated earlier.

Table 19. ET_A Test Set[a]

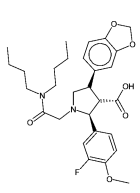

33

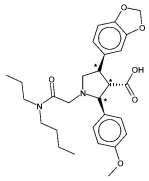

34

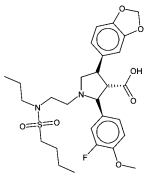

35

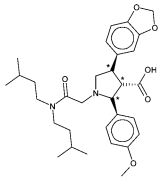

(±)-36

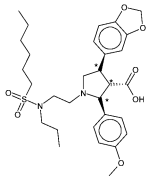

(±)-37

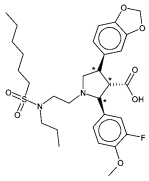

(±)-38

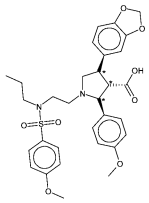

(±)-39

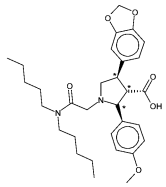

(±)-40

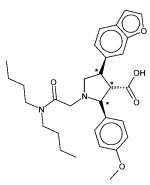

(±)-41

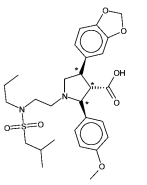

(±)-42

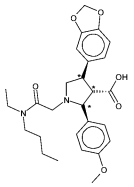

(±)-43

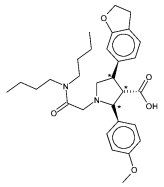

(±)-44

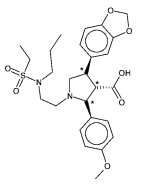

(±)-45

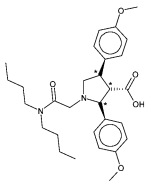

(±)-46

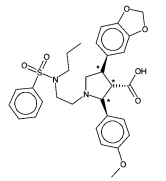

(±)-47

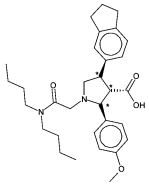

(±)-48

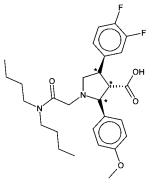

(±)-49

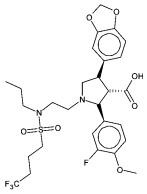

50

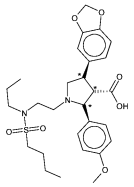

(±)-51

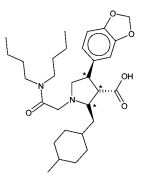

(±)- 52

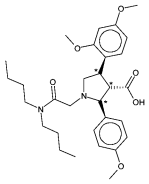

(±)-53

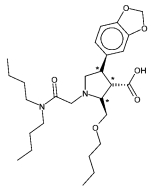

(±)-54

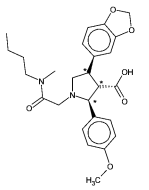

(±)-55

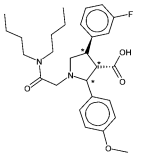

(±)-56

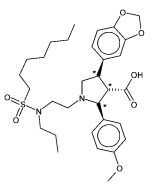

(±)-57

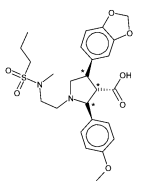

(±)-58

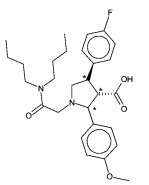

(±)-59

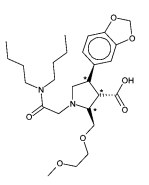

(±)-60

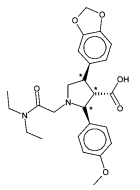

(±)-61

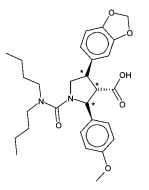

(±)- 62

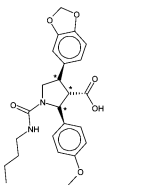

(±)-63

[a] The * means that the centers keep the relative stereochemistry and they are racemic mixtures as indicated by (±). The unmarked compounds are enantiopure and possess the drawn stereochemistry.

The training set is presented in Table 18. A 31-compound test set has been selected in order to test the predictive capability of the model, presented in Table 19.

The IC_{50} values of the training set lie between 0.07 and 14 000 nM, which is over 6 orders of magnitude, and those of the test set lie between 0.16 and 684 nM, which is over 3 orders of magnitude. The results of different conditions in pharmacophore generation are shown in Table 20.

Both hypotheses using TRUE and FALSE (**XVII** and **XVIII**) present results of very similar quality. With the FALSE value, the Δ cost is slightly higher, but with TRUE, the RMS value and correlation are a little bit better.

Table 20. Best Hypothesis Data for the ET_A Receptor

hypothesis	conditions[a]	Δ cost	RMS	correlation	features[b]
XVII	FALSE	97.072	1.1506	0.9223	HBA, HyAl, HyAr, PosIo, NegIo
XVIII	TRUE	96.737	1.0984	0.9309	HBA, HyAl, HyAr, PosIo, NegIo

[a] FALSE/TRUE: value of the compare.scaledMultiBlobFeatureErrors parameter. [b] PosIo stands for positive ionizable.

Table 21. Results for Scoring the Best ET_A Hypotheses against the Training Set

	compare.scaledMultiBlobFeatureErrors			
	FALSE		TRUE	
hypothesis	score	correlation	score	correlation
XVII	1.1507	0.9223	1.3397	0.9005
XVIII	1.6530	0.8778	1.0993	0.9309

Table 22. Results for Scoring the Best ET_A Hypotheses against the Test Set

	compare.scaledMultiBlobFeatureErrors			
	FALSE		TRUE	
hypothesis	score	correlation	score	correlation
XVII	1.4887	0.7247	1.5119	0.6662
XVIII	2.6419	0.5868	1.7145	0.6091

Table 23. Prediction of the Affinity and Error Reported during Automatic Hypothesis Generation of Hypothesis **XVII**[a]

name	actual	estimated	error
2	0.07	0.021	−3.4
3	0.14	0.150	1.1
4	0.31	2.000	6.4
5	0.48	2.000	4.2
6	0.55	2.500	4.6
7	0.60	5.000	8.4
8	0.66	0.680	1.0
9	1.00	1.500	1.5
10	1.60	6.500	4.1
11	1.90	2.600	1.4
12	2.00	4.500	2.2
13	2.30	1.200	−1.9
14	2.50	4.900	2.0
15	4.60	3.900	−1.2
16	5.20	16.000	3.0
17	5.60	44.000	7.9
18	8.10	5.900	−1.4
19	9.20	6.600	−1.4
20	10.00	5.300	−1.9
21	20.00	3.300	−6.0
22	88.00	110.000	1.2
23	110.00	140.000	1.3
24	130.00	120.000	−1.1
25	170.00	9.100	−19.0
26	450.00	150.000	−3.0
27	520.00	420.000	−1.2
28	770.00	63.000	−12.0
29	1200.00	4700.000	3.8
30	2000.00	650.000	−3.1
31	6800.00	2600.000	−2.7
32	14000.00	3000.000	−4.7

[a] Estimated means the estimated affinity, and actual means the experimentally determined affinity (nM).

Next, the best hypotheses were scored against the training set considering both values possible for the compare.scaledMultiBlobFeatureErrors parameter (Table 21).

Now, the overall best hypothesis is **XVIII**, using TRUE, which was the second best hypothesis with regard to the Δ cost value. Hypothesis **XVII** (FALSE) is the second best now, with similar results as those of **XVIII**. To verify the predictive capability of the hypotheses, they were scored against the test set shown in Table 19. The results are presented in Table 22.

Table 24. Prediction Data of the Best ET_A Hypothesis (**XVII**) against the Test Set with compare.scaledMultiBlobFeatureErrors Set to FALSE[a]

name	actual	estimated	error
33	0.16	3.60	23.0
34	0.22	2.80	13.0
35	0.38	0.87	2.3
36	0.43	5.00	12.0
37	0.43	3.40	8.0
38	0.46	1.70	3.7
39	0.53	7.60	14.0
40	0.56	2.30	4.2
41	0.70	10.00	14.0
42	0.78	1.40	1.7
43	0.85	7.10	8.3
44	1.00	3.10	3.1
45	1.20	2.90	2.4
46	1.30	12.00	9.4
47	1.40	4.60	3.3
48	1.50	11.00	7.6
49	1.50	2.00	1.3
50	1.66	3.60	2.2
51	2.00	4.50	2.3
52	3.60	4.20	1.2
53	3.70	12.00	3.1
54	4.10	6.30	1.5
55	4.71	3.50	−1.4
56	5.00	1.90	−2.7
57	5.10	1.70	−3.0
58	10.00	0.94	−11.0
59	14.00	2.70	−5.1
60	24.60	4.40	−5.5
61	32.90	75.00	2.3
62	396.00	2700.00	6.9
63	684.00	1500.00	2.2

[a] Estimated means the estimated affinity, and actual means the experimentally determined affinity (nM).

The best hypothesis in scoring against the test set is **XVII**, as was the case with regard to the Δ cost value during the automatic pharmacophore model generation, making it appear as the overall best hypothesis.

Table 23 presents the affinity estimation and error values of the training set using the best pharmacophore obtained (**XVII**), while Table 24 presents the affinity prediction and error of the test set using the same pharmacophore model.

The error is calculated as the ratio between the estimated and the actual affinity. When this value is positive, it means that the affinity is overestimated; when it is negative, the affinity is underestimated. Thus, a value of −1.3 means that the estimated affinity is 30% lower than the actual affinity, and 1.0 means no error. There are no values between −1.0 and 1.0, as can be seen in Table 23. The predictability of hypothesis **XVII** is quite good. All but two of the compounds included in the training set have an error lower than 10, which means that the affinity prediction of these compounds

Table 25. ET_B Training Set[a]

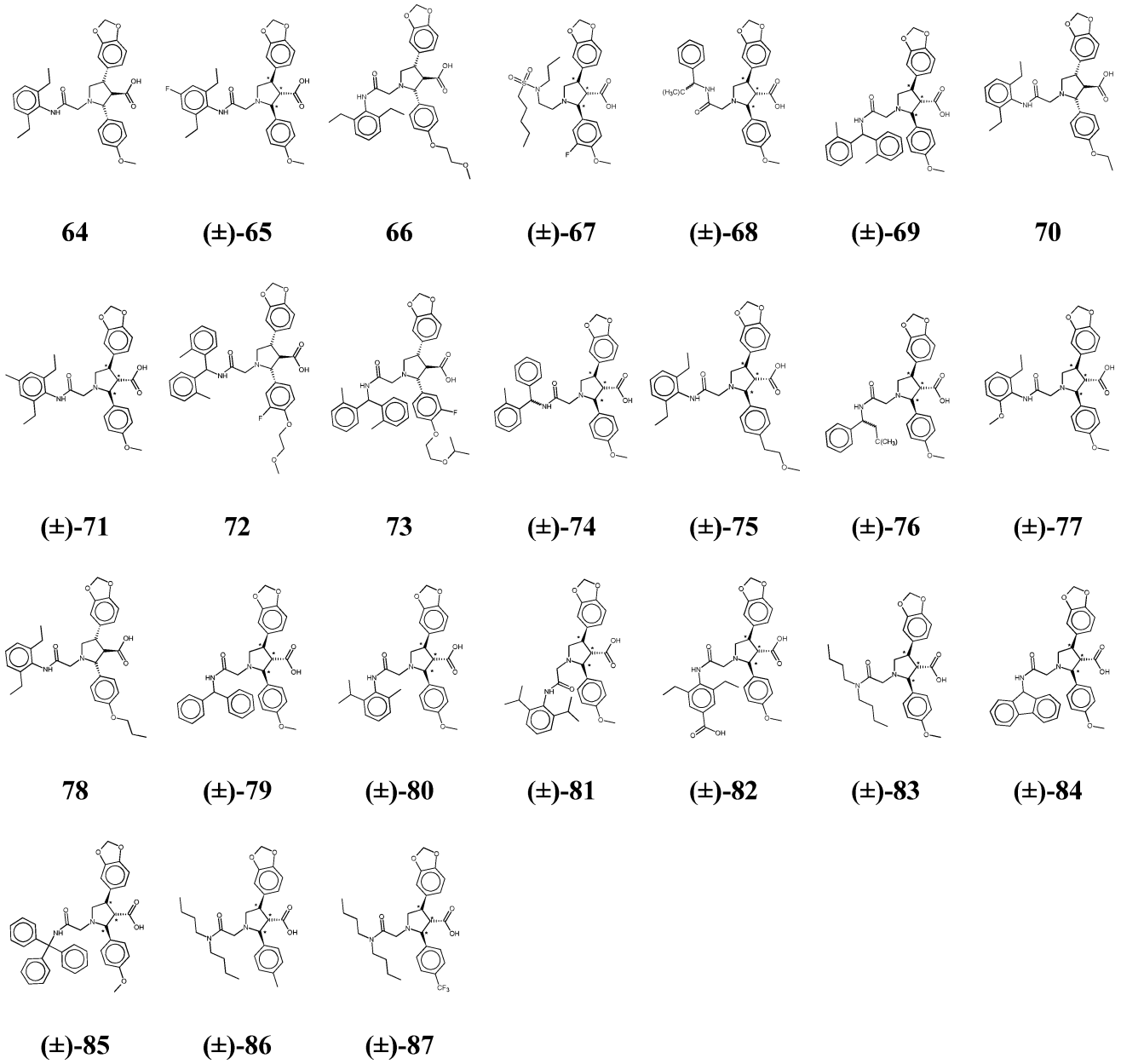

[a] The * means that the centers keep the relative stereochemistry and they are racemic mixtures as indicated by (±). The unmarked compounds are enantiopure and possess the drawn stereochemistry.

falls between 10-fold greater and $^1/_{10}$ of the actual affinity, and the two compounds with the highest error are among the lowest active.

Figure 5 shows hypothesis **XVII** fitted by the most active enantiomerically pure compound (**3**). The carboxylic acid maps the negative ionizable feature; the amino group of the pyrrolidine ring is placed onto the positive ionizable feature, and one oxygen from the sulfonamide maps the hydrogen-bond acceptor feature. The side chain maps the hydrophobic aliphatic feature, while the aromatic ring attached to the pyrrolidine ring is placed onto the hydrophobic aromatic feature.

Table 24 shows the prediction data of the best ET_A hypothesis against the test set. Only 6 out of 31 compounds possess an error value higher than 10. Regarding the data presented up to now, we can see that **XVII** is the hypothesis that presents the highest prediction capability for compounds in both the training and test sets.

MODELS FOR THE ET_B RECEPTOR

A 25-compound training set (presented in Tables 25 and 26) was carefully selected from the literature[12,18] according to the general guidelines explained earlier. The IC_{50} values were obtained from the same literature sources. The IC_{50} values of the training set range from 0.27 to 14 300 nM (5 orders of magnitude). A 26-compound test set was selected from the same literature source, and its activity range was from 1 to 1790 nM (more than 3 orders of magnitude) and is presented in Tables 27 and 28.

As it can be seen in Table 29, all the Δ cost values in the ET_B hypothesis are considerably lower than the ones in the

Table 26. Prediction of the Affinity and Error Reported during Automatic Hypothesis Generation of Hypothesis **XX**[a]

name	actual	estimated	error
64	0.27	0.26	−1.10
35	0.60	5.10	8.40
65	0.80	0.30	−2.70
66	0.85	0.70	−1.20
67	0.85	3.60	4.30
68	0.94	0.64	−1.50
69	1.10	5.80	5.30
70	1.20	5.50	4.60
71	1.20	2.60	2.20
72	1.70	2.70	1.60
73	1.90	5.90	3.10
74	3.40	12.00	3.40
75	3.80	4.10	1.10
76	5.00	21.00	4.20
77	5.80	3.80	−1.50
78	6.40	3.80	−1.70
79	8.10	31.00	3.80
80	20.00	7.70	−2.60
81	26.00	2.80	−9.10
82	44.00	11.00	−4.10
83	520.00	340.00	−1.50
84	600.00	150.00	−4.00
85	740.00	170.00	−4.40
86	2100.00	1700.00	−1.30
87	14000.00	1200.00	−12.00

[a] Estimated means the estimated affinity, and actual means the experimentally determined affinity (nM).

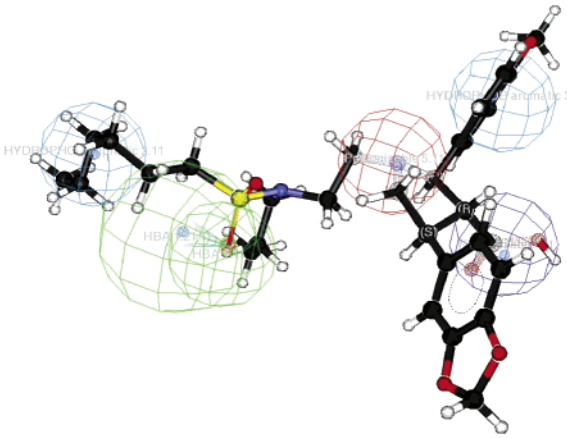

Figure 5. Best ET_A hypothesis (**XVII**) aligned with the most active enantiomerically pure compound (**3**). Dark blue, NegIo; red, PosIo; blue, HyAl and HyAr; green, HBA. PosIo stands for positive ionizable.

ET_A hypothesis. While the Δ cost values in the ET_A hypothesis are around 90 bits, the Δ cost values of the ET_B hypothesis lie between 42 and 50 bits. Thus, there is only a 75−90% possibility that the ET_B hypotheses present a true correlation.

According to the results presented in Table 30, **XX**, with the standard features and the TRUE value for the compare.scaledMultiBlobFeatureErrors parameter, shows the

Table 27. ET_B Test Set[a]

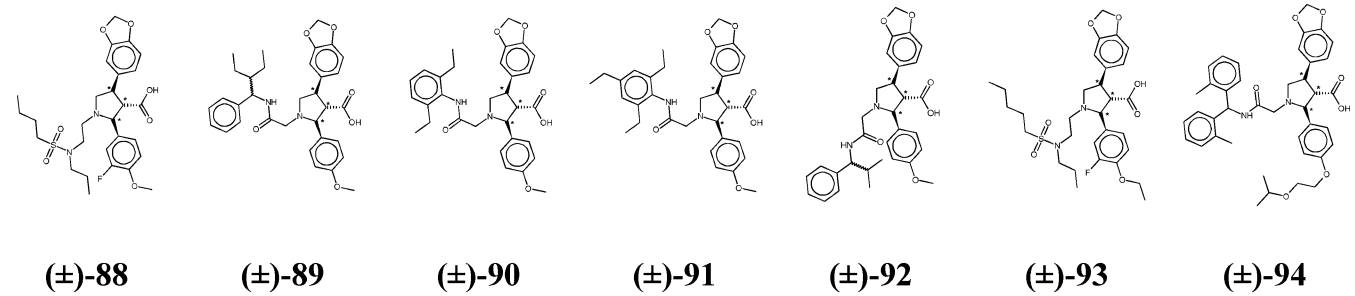

(±)-88 **(±)-89** **(±)-90** **(±)-91** **(±)-92** **(±)-93** **(±)-94**

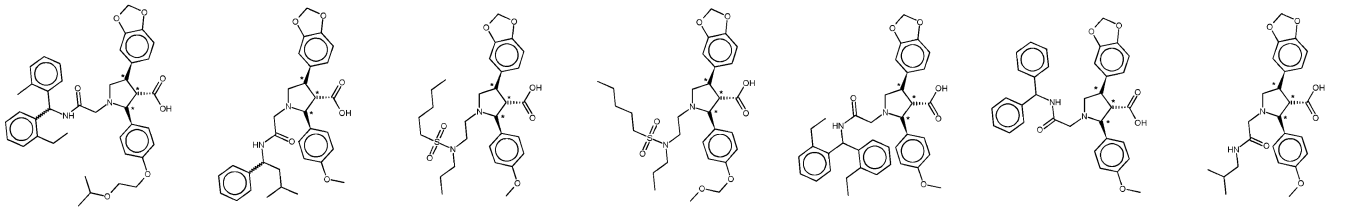

(±)-95 **(±)-96** **(±)-97** **(±)-98** **(±)-99** **(±)-100** **(±)-101**

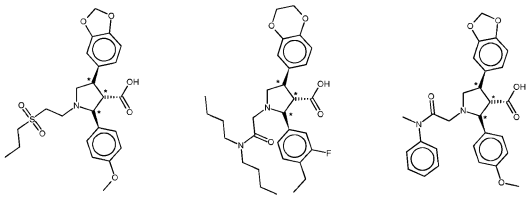

(±)-102 **(±)-103** **(±)-104**

[a] The * means that the centers keep the relative stereochemistry and are racemic mixtures as indicated by (±). The unmarked compounds are enantiopure and possess the drawn stereochemistry.

Table 28. Prediction Data of the Best ET_B Hypothesis (**XX**) against the Test Set with compare.scaledMultiBlobFeatureErrors Set to FALSE[a]

name	actual	estimated	error
88	1.00	8.60	8.60
89	1.10	12.00	11.00
3	1.12	12.00	11.00
5	1.28	6.30	4.90
90	1.40	8.10	5.80
50	1.46	38.00	26.00
91	1.50	9.60	6.40
92	2.10	14.00	6.90
93	2.60	19.00	7.30
94	3.30	0.84	−3.90
95	3.30	15.00	4.60
96	3.40	110.00	31.00
97	4.10	8.10	2.00
41	5.00	20.00	3.90
98	5.20	9.90	1.90
42	5.20	21.00	4.00
99	6.60	8.30	1.30
48	8.00	340.00	43.00
20	34.00	16.00	−2.10
10	36.00	7.80	−4.60
100	108.00	97.00	−1.10
101	184.00	1600.00	8.90
102	750.00	77.00	−9.80
105	950.00	2000.00	2.10
104	1180.00	3000.00	2.60
55	1390.00	2000.00	1.40

[a] Estimated means the estimated affinity, and actual means the experimentally determined affinity (nM).

highest correlation for the training set. Again, the best results are obtained using the same settings as those used during automatic pharmacophore generation.

The results of scoring the best hypotheses against the test set are presented in Table 31. The highest correlation is that of hypothesis **XX**, the same case with the highest Δ cost value.

In Table 26, the actual and estimated activities of the training set for hypothesis **XX** are shown. Only 1 out of 25 compounds has an error in affinity estimation higher that 10, and this is the compound with the lowest affinity. Thus, it can be stated that the correlation of the training set is quite good.

Thus, we chose **XX** as being the best hypothesis. Now, the best hypothesis is using TRUE, while in ET_A, it was using FALSE.

Table 28 shows the data for scoring the best hypothesis against the test set. It can be stated that, despite the low Δ cost value, the predictability of the hypotheses is high. Only 5 out of 26 compounds show an error in the prediction of the affinity higher than 10.

Figure 6 depicts the most active compound (**64**) in the training set aligned to the best hypothesis (**XX**). The positive ionizable feature is mapped by the amino group of the pyrrolidine ring, and the negative ionizable feature is mapped by the carboxylic group. The hydrogen-bond acceptor is mapped by the phenyl ether group, while both hydrophobic features (aromatic and aliphatic) are mapped by the largest side chain of the compound.

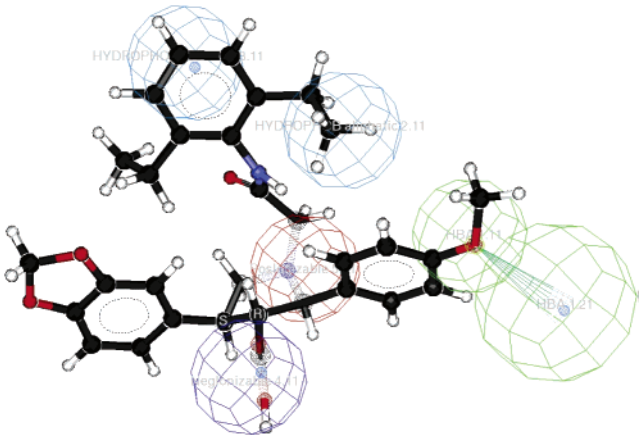

Figure 6. Best ET_B hypothesis (**XX**) with compound **64**, the most active ET_B antagonists, aligned to it. Dark blue, NegIo; blue, HyAr and HyAl; gray, HBA.

COMPARISON OF PHARMACOPHORE MODELS FOR ET_A AND ET_B

When comparing the affinity values of the tested compounds toward the two different ET receptor subtypes, it becomes apparent that many compounds possess a rather low ET_A/ET_B selectivity. Table 32 shows the affinity data of the ET_B training set toward both the ET_B and ET_A receptors. Among the most active sets (entries in italics in Table 32), some compounds are even more active as ET_A antagonists than as ET_B antagonists. Among the most active compounds used to build the hypotheses, only three are more than 1000-fold more active as ET_B antagonists than as ET_A antagonists. Only three more are ET_B-selective by a factor of 100 or more.

To state the ability of these pharmacophores to discriminate between both subtypes, we studied the activity prediction of both best pharmacophores, **XVII** (ET_A) and **XX** (ET_B), scoring the hypotheses against both test sets. A summary of the data is shown in Table 33. In Table 33, it can be seen that hypothesis **XX** describes reasonably well the ET_A test set, but **XVII** is not able to describe the ET_B test set. Then, it is clear that pharmacophore **XVII** is selective only to ET_A antagonists, while **XX** is not selective at all between both subtypes.

We furthermore tested whether our models are able to retrieve entries from the WDI database which are described as endothelin antagonists. To do so, we searched for entries with the keywords "ENDOTHELIN-ANTAGONIST", "ENDOTHELIN-A-ANTAGONIST", "ENDOTHELIN-B-ANTAGONIST", "ENDOTHELIN-RECEPTOR-LIGAND", and "endothelin-1-inhibitor" in either the "Activity Keywords" or the "Mode of Action" fields. Of the 160 retrieved compounds, 143 showed a molecular weight below 700. Of

Table 29. ET_B Best Hypothesis Reported[a]

hypothesis	conditions	Δ cost	RMS	correlation	features
XIX	FALSE	47.340	1.289	0.8707	HBA, HyAl, HyAr, PosIo, NegIo
XX	TRUE	49.100	1.141	0.9051	HBA, HyAl, HyAr, PosIo, NegIo

[a] FALSE/TRUE: value of the compare.scaledMultiBlobFeatureErrors parameter.

Table 30. Results for Scoring the Best ET_B Hypotheses against the Training Set

	compare.scaledMultiBlobFeatureErrors			
	FALSE		TRUE	
hypothesis	score	correlation	score	correlation
XIX	1.2895	0.8707	1.7854	0.7997
XX	1.4465	0.8743	1.1414	0.9051

Table 31. Results for Scoring the Best ET_B Hypotheses against the Test Set

	compare.scaledMultiBlobFeatureErrors			
	FALSE		TRUE	
hypothesis	score	correlation	score	correlation
XIX	1.7974	0.6179	1.7793	0.5621
XX	1.7203	0.7840	1.5534	0.7209

Table 32. ET_B Training Set Affinity Data as ET_A and ET_B Antagonist[a]

name	ET_A	ET_B	ET_A/ET_B
64	89.00	0.27	329.63
35	0.38	0.60	0.63
65	22.00	0.80	27.50
66	3700.00	0.85	4352.94
67	0.52	0.85	0.61
68	8.80	0.94	9.36
69	161.00	1.10	146.36
70	340.00	1.20	283.33
71	18.00	1.20	15.00
72	27014.00	1.70	15890.59
73	51703.00	1.90	27212.11
74	63.50	3.40	18.68
75	11000.00	3.80	2894.74
76	131.00	5.00	26.20
77	200.00	5.80	34.48
78	8200.00	6.40	1281.25
79	45.90	8.10	5.67
80	100.00	20.00	5.00
81	920.00	86.00	10.70
82	840.00	44.00	19.09
83	0.36	515.00	6.99×10^{-4}
84	1228.00	600.00	2.05
85	432.00	744.00	0.58
86	0.12	2140.00	5.60×10^{-5}
87	0.33	14300.00	2.31×10^{-5}

[a] Higher numbers for ET_A/ET_B mean higher selectivity as ET_B antagonists.

Table 33. Comparison of the Results of Scoring the ET_A and ET_B Test Set against the Pharmacophores **XVII** and **XX**

		compare.scaledMultiBlobFeatureErrors			
		FALSE		TRUE	
hypothesis	test set	score	correlation	score	correlation
XVII	ET_A	1.5118	0.6662	1.4987	0.7247
XX	ET_A	3.7909	0.5727	4.4850	0.5431
XVII	ET_B	3.0994	0.0615	2.7893	0.0718
XX	ET_B	1.5534	0.7209	1.7203	0.7840

these, 53 are marked as "ENDOTHELIN-A-ANTAGONIST" and 14 as "ENDOTHELIN-B-ANTAGONIST". These last two lists overlap, because nine compounds have entries for both subtypes. These lists were searched with both the quantitative (**XII**) and qualitative (**XXI**) models from ref 6, as well as with our quantitative ET_A (**XVII**) and ET_B (**XX**) models. Additionally, we calculated the enrichment for each of these searches, being defined as the ratio of the active compounds in the hit list to the number of compounds in the hit list over the active compounds in the database to the total number of compounds in the database. The results of this search are summarized in Table 34.

Table 34. Search Results for Subsets of the Derwent WDI, Comprised of Compounds Marked as Endothelin Antagonists by Their 1D Properties

	number of hits				enrichment (%)		
hypothesis	total	ET all[a]	ET_A	ET_B	ET all[a]	ET_A	ET_B
entire database	63307	160	55	17			
MW < 700		143	53	14			
XII (ET_A quant.)[6]	1083	78	36	11	39.7	31.9	45.9
XXI (ET_A qual.)[6]	606	43	20	7	39.4	31.4	52.2
XVII (ET_A quant.)	103	14	7	3	81.2	60.2	131.7
XX (ET_B quant.)	442	6	2	2	5.4	6.0	20.5

[a] All endothelin antagonist, both with and without specified subtype affinity.

As can be seen from Table 34, both literature models retrieve more of the active compounds, while our ET_A hypothesis **XVII** shows the highest enrichment factors. From the fact that the highest enrichment values are found when searching the ET_B subset, we can also see that none of the ET_A hypotheses manage to discriminate between ET_A and ET_B antagonists. This higher enrichment for ET_B is reflected to an even higher extent for our ET_B hypothesis—as should be expected—but because of the low total number of actives retrieved, we may not draw any conclusions from this. Visual inspection of the 143 endothelin antagonists showed that many of these compounds do not bear the 3-carboxypyrrolidine moiety that is present in all of our test and training compounds and that they also lack either the positive or negative ionizable feature, or both. To assess the selectivity of our hypotheses for the group of 3-carboxypyrrolidines, we further narrowed our search to only those compounds of the WDI with both a known endothelin receptor affinity and this substructure. We found, in total, 12 compounds, of which six had a reported affinity for ET_A and three had a reported affinity for ET_B. All three ET_A hypotheses were able to retrieve all 12 compounds. The ET_B hypothesis **XX** found six of the total list of 12 and two compounds for both the ET_A and the ET_B subset. One compound which had a reported affinity for both subtypes was present in both of the later result lists.

With respect to the spatial orientation of the pharmacophore models, it is surprising that, apart from the position of the positive and negative ionizable features, the two final models look quite different from each other. Figure 7 shows some views of the final pharmacophore models for the ET_A and ET_B receptor antagonists: In Figure 7a, both pharmacophore models, oriented similarly in space with regard to the negative and positive ionizable features, are shown. When both pharmacophore models are placed in this orientation, it is easy to compare the differences between the two hypotheses. Figure 7b shows an overlay of both pharmacophore models. In Figure 7c, both pharmacophore models are fitted by their most active compound from both training sets.

The first important point comparing both pharmacophore models is that, in the ET_B receptor hypothesis, the hydrogen-bond acceptor is mapped by one oxygen atom from the dioxolane bound to the aromatic ring. But in the ET_A receptor

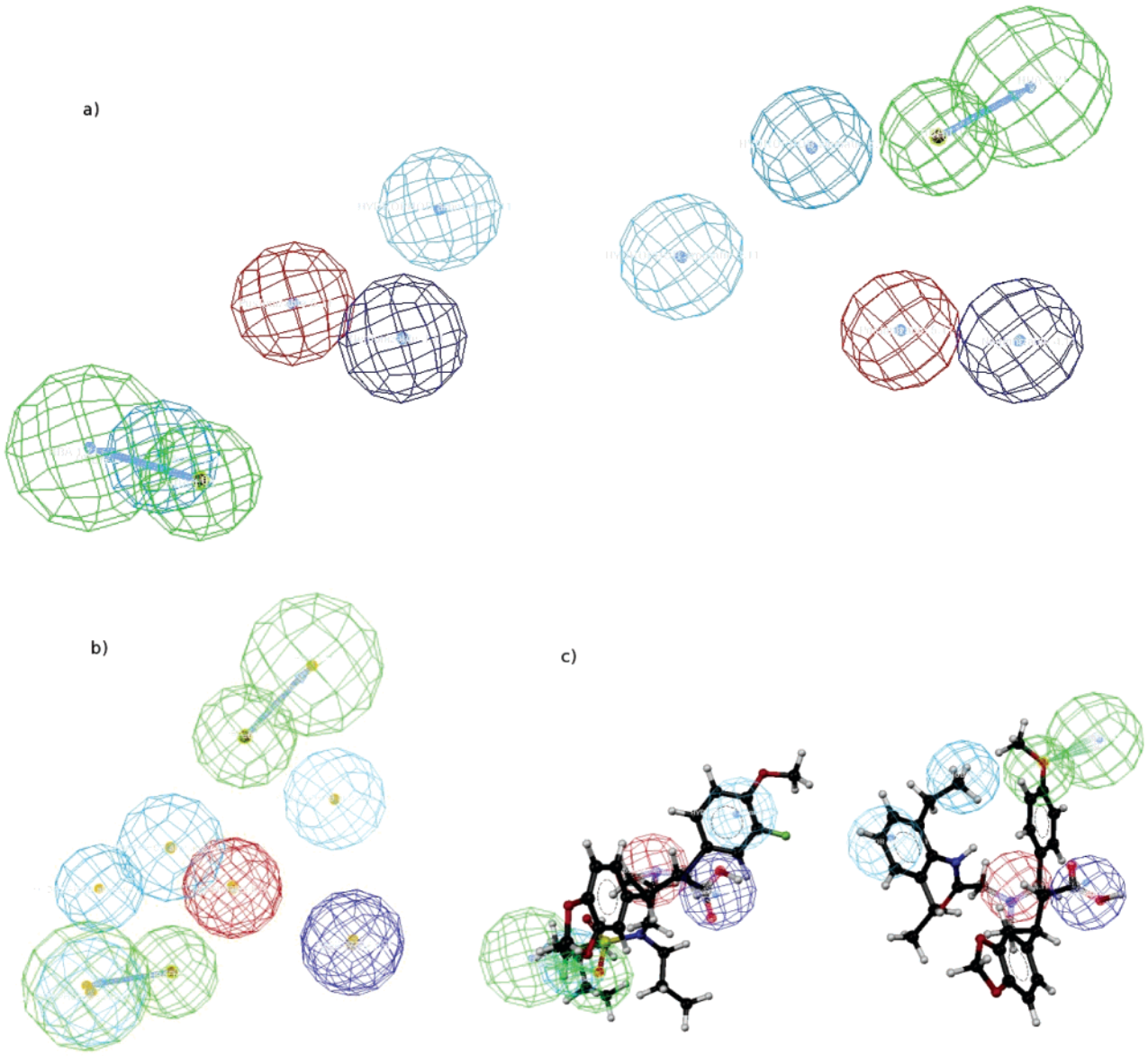

Figure 7. (a) Best ET_A and ET_B antagonist receptor pharmacophore models side by side. (b) ET_A and ET_B antagonist receptor pharmacophore models overlaid. (c) ET_A and ET_B antagonist receptor pharmacophore models aligned with **3** and **65**, respectively.

hypothesis, the hydrogen-bond acceptor is mapped by an oxygen atom of the sulfonamide moiety. This means that the putative binding sites of the ET_B and ET_A antagonist may present different locations for hydrogen-bond donors.

The second main difference between the ET_A and ET_B receptor models is the position of the hydrophobic aromatic features. In the ET_B receptor model, the hydrophobic aromatic feature is fitted by the side chain linked to the nitrogen atom of the pyrrolidine ring, while in the ET_A receptor antagonist pharmacophore, the hydrophobic aromatic feature is fitted by the aromatic residues linked to position 2 of the pyrrolidine ring. Finally, the hydrophobic aliphatic feature in both models is found at different positions. When these differences are compared to the SAR presented by Jae et al.,[12] the importance of the position of the hydrogen-bond acceptor is highlighted. Other differences may be masked by both the limitation of the Catalyst package that includes only up to five features for hypotheses generated with HypoGen and by the fact that the requirements for the data for HypoGen models (same assay, large spread of affinity data) were only met by compounds from one structural class (pyrrolidine-3-carboxylic acid derivatives).

When the ET_A hypothesis **XVII** is compared to the previous ET_A hypothesis published by our research group,[6] some difference can be found. While the previous hypotheses present two hydrophobic features, one bond acceptor, one ring aromatic, and one negative ionizable, the new pharmacophore model presents the hydrophobic features separated into one aromatic and one aliphatic and no ring aromatic. On the other hand, the present ET_A pharmacophore model presents one positive ionizable that does not appear in the previous hypothesis.

CONCLUSIONS

In this work, the influence of the compare.scaledMultiBlobFeatureErrors parameter on pharmacophore model generation, affinity estimation, and database searching within Catalyst has been studied. It was found that different versions of the program can lead to different pharmacophore models, the retrieved pharmacophore models being different in type

and number of features or their spatial arrangement. Using the FALSE value tends to retrieve pharmacophore models with better statistical quality than those using the TRUE value. On the other hand, TRUE is always better for database searching and affinity prediction. Then, the data obtained from different program versions should be compared carefully.

We have built two quantitative pharmacophore models for the ET_A and ET_B receptor antagonists applying the HypoGen algorithm in Catalyst. Both receptor pharmacophore models present the same five features (one hydrogen-bond acceptor, one negative and one positive ionizable, one hydrophobic aromatic, and one hydrophobic aliphatic feature), although these features are mapped by different moieties of the investigated compounds.

The quality of the pharmacophore models was investigated by comparing the score and correlation values retrieved for a test set. A comparison of the best pharmacophore models for both ET receptor subtypes showed that especially the positions of the hydrophobic aromatic and the hydrogen-bond acceptor features seem to play an important role for subtype selectivity. Pharmacophore model **XVII** was able to discriminate between both subtypes, while hypothesis **XX** has low selectivity for both subtypes; this may be due to the fact that the ET_B antagonists used during the generation of pharmacophore model **XX** present too low of a selectivity to both subtypes.

EXPERIMENTAL SECTION

All of this study was performed using Catalyst 4.9 installed on a Silicon Graphics Octane workstation equipped with a 300 MHz MIPS RISC R12000 processor and 1GB of RAM running the Irix64 6.5 operating system.

ACKNOWLEDGMENT

The authors thank Mag. Dr. E. M. Kleinrath and Dr. O. Funk for their dedicated support. J.R.C.G. offers thanks for the grant from Ministerio de Ciencia y Tecnología associated with the project BQU2001-2600.

REFERENCES AND NOTES

(1) Krovat, E. M.; Langer, T. Non-Peptide Angiotensin II Receptor Antagonists: Chemical Features Based Pharmacophore Identification. *J. Med. Chem.* **2003**, *46*, 716−726.

(2) Langer, T.; Krovat, E. M. Chemical Feature-Based Pharmacophores and Virtual Library Screening for Discovery of New Leads. *Curr. Opin. Drug Discovery Dev.* **2003**, *6* (3), 370−376.

(3) Accelrys Inc, San Diego, CA. www.accelrys.com (accessed Dec 2005).

(4) This parameter represents the maximum number of omitted features allowed for the compare operation with the FAST algorithm. The default value −1 considers all mappings even if one or more features do not fit in the compound.

(5) Debnath, A. K. Pharmacophore Mapping of a Series of 2,4-Diamino-5-deazapteridine Inhibitors of *Mycobacterium avium* Complex Dihydridrofolate Reductase. *J. Med. Chem.* **2001**, *45*, 41−53.

(6) Funk, O. F.; Kettmann, V.; Drimal, J.; Langer, T. Chemical Function Based Pharmacophore Generation of Endothelin-A Selective Receptor Antagonists. *J. Med. Chem.* **2004**, *47*, 2750−2760.

(7) Li, R.; Sirawaraporn, R.; Chitnumsub, P.; Sirawaraporn, W.; Wooden, J.; Athappilly, F.; Turley, S.; Hol, W. G. J. Three-Dimensional Structure of *M. tuberculosis* Dihydrofolate Reductase Reveals Opportunities for the Design of Novel Tuberculosis Drugs. *J. Mol. Biol.* **2000**, *295*, 307−323.

(8) Kharkar, P. S.; Kulkarni, V. M. A Proposed Model of *Mycobaterium avium* Complex Dihydrofolate Reductase and Its Utility for Drug Design. *Org. Biomol. Chem.* **2003**, *1*, 1315−1322.

(9) Wolber, G.; Langer, T.; LigandScout: 3-D Pharmacophores Derived from Protein-Bound Ligands and Their Use as Virtual Screening Filters. *J. Chem. Inf. Model.* **2005**, *45* (1), 160−169.

(10) Yanagisawa, M.; Kurihara, H.; Kimura, S.; Tomobe, Y.; Kobayashi, M.; Mitsui, Y.; Yazaki, Y.; Goto, K.; Masaki, T. Novel Potent Vasoconstrictor Peptide Produced by Vascular Endothelin Cells. *Nature* **1988**, *332*, 411−415.

(11) (a) Satoh, T.; Barlow, D. Molecular Modelling of the Structures of Endothelin Antagonists Identification of a Possible Structural Determinant for ET-A Receptor Binding. *FEBS Lett.* **1992**, *310* (1), 83−87. (b) Krystek, S. R.; Hunt, J. T.; Stein, P. D.; Stouch, T. R. Three-Dimensional Quantitative Structure−Activity Relationships of Sulfonamide Endothelin Inhibitors. *J. Med. Chem.* **1995**, *38*, 656−668. (c) Chen, Q.; Wu C.; Maxwell, D.; Krudy, G. A.; Dixon, R. A. F.; You, T. J. A 3D QSAR Analysis of in Vitro Binding Affinity and Selectivity of 3-Isoxazolylsulfonylaminothiophenes as Endothelin Receptor Antagonists *Quant. Struct.-Act. Relat.* **1999**, *18*, 124−133.

(12) Jae, H. S.; Winn, M.; von Geldern, T. W.; Sorensen, B. K.; Chiou, W. J.; Nguyen, B.; Marsh, K. C.; Opgenorth, T. J. Pyrrolidine-3-carboxylic Acids as Endothelin Antagonists. 5. Highly Selective, Potent and Orally Active ETA Antagonists. *J. Med. Chem.* **2001**, *44*, 3978−3984.

(13) http://www.accelrys.com/support/life/Catalyst/confanal.html and http://www.accelrys.com/support/life/Catalyst/catbest.html.

(14) Reference deleted in press.

(15) Smellie, A.; Teig, S. L.; Towbin, P. Poling: Promoting Conformational Variation. *J. Comput. Chem.* **1995**, *16*, 171−187.

(16) Kirchmair, J.; Laggner, C.; Wolber, G.; Langer, T. Comparative Analysis of Protein-Bound Ligand Conformations with Respect to Catalyst's Conformational Space Subsampling Algorithms. *J. Chem. Inf. Model.* **2005**, *45* (2), 422−430.

(17) This parameter affects compare/fit operations from graphical interface and citest. This parameter is similar to the catHypo.forceAbsoluteStereochemistry parameter used in HypoGen and HipHop. The default value is 1.

(18) (a) Winn, M.; von Geldern, T. W.; Opgenorth, T. J.; Jae, H. S.; Tasker, A. S.; Boyd, S. A.; Kester, J. A.; Mantei, R. A.; Bal, R.; Sorensen, B, K.; Wu-Wong, J. R.; Chiou, W. J.; Dixon, D. B.; Novosad, E. I.; Hernandez, L.; Marsh, K. C. 2,4-Diarylpyrrodine-3-carboxilic Acids−Potent ET_A Selective Endothelin Receptor Antagonists. 1. Discovery of A-127722. *J. Med. Chem.* **1996**, *39*, 1039−1048. (b) Tasker, A. S.; Sorensen, B. K.; Jae, H. S.; Winn, M.; von Geldern, T. W.; Dixon, D. B.; Chiou, W. J.; Dayton, B. D.; Calzadila, S.; Hernandez, L.; Marsh, K. C.; WuWong, J. R.; Opgenorth, T. J. Potent and Selective Non-Benzodioxole-Containing Endothelin-A Receptor Antagonists. *J. Med. Chem.* **1997**, *40*, 322−330. (c) Jae, H. S.; Winn, M.; Dixon, D. B.; Marsh, K. C.; Nguyen, B.; Opgenorth, T. J.; von Geldern, T. W. Pyrrolidine-3-carboxylic Acids as Endothelin Antagonists. 2. Sulfonamide-Based ET_A/ET_B Mixed Antagonists. *J. Med. Chem.* **1997**, *40*, 3217−3227. (d) von Geldern, T. W.; Tasker, A. S.; Sorensen, B. K.; Winn, M.; Szczepankiewicz, B. G.; Dixon, D. B.; Chiou, W. J.; Wang, L.; Wessale, J. L.; Adler, A.; Marsh, K. C.; Nguyen, B.; Opgenorth, T. J. Pyrrolidine-3-carboxylic Acids as Endothelin Antagonists. 4. Side Chain Conformational Restriction Leads to ET_B Selectivity. *J. Med. Chem.* **1999**, *42*, 3668−3678. (e) Liu, G.; Kozmina, N. S.; Winn, M.; von Geldern, T. W.; Chiou, W. J.; Dixon, D. B.; Nguyen, B.; Marsh, K. C.; Opgenorth, T. J. Design, Synthesis and Activity of a Series of Pyrrolidine-3-carboxylic Acid-Based, Highly Specific, Orally Active ETB Antagonists Containing a Diphenylmethylamine Acetamide Side Chain. *J. Med. Chem.* **1999**, *42*, 3679−3689. (f) Boyd, S. A.; Mantei, R. A.; Tasker, A. S.; Liu, G.; Sorensen, B. K.; Henry, K. J., Jr.; von Geldern, T. W.; Winn, M.; Wu-Wong, J. R.; Chiou, W. J.; Dixon, D. B.; Hutchins, C. W.; Marsh, K. C.; Nguyen, B.; Opgenorth, T. J. Discovery of a Series of Pyrrolidine-Based Endothelin Receptor Antagonists with Enhanced ETA Receptor Selectivity. *Bioorg. Med. Chem.* **1999**, *7*, 991−1002.

CI060006T